HHS Public Access

Author manuscript

Nat Struct Mol Biol. Author manuscript; available in PMC 2016 October 11.

Published in final edited form as:

Nat Struct Mol Biol. 2016 May ; 23(5): 402–408. doi:10.1038/nsmb.3207.

Resolving individual steps of Okazaki fragment maturation at msec time-scale

Joseph L. Stodola and **Peter M. Burgers**

Department of Biochemistry and Molecular Biophysics, Washington University School of Medicine, Saint Louis, Missouri, USA

Abstract

DNA polymerase delta (Pol δ) is responsible for elongation and maturation of Okazaki fragments. Pol δ and flap-endonuclease FEN1, coordinated by the PCNA clamp, remove RNA primers and produce ligatable nicks. We have studied this process with the *Saccharomyces cerevisiae* machinery at msec resolution. During elongation, PCNA increased the catalytic rate of Pol δ by >30-fold. When Pol δ invaded double-stranded RNA-DNA representing unmatured Okazaki fragments, the incorporation rate of each nucleotide decreased successively to 10–20% of the preceding nucleotide. Thus, the nascent flap acts as a progressive molecular brake on the polymerase, and consequently, FEN1 cuts predominantly single nucleotide flaps. Kinetic and enzyme trapping experiments support a model in which a stable PCNA-DNA-Pol δ-FEN1 complex moves processively through the iterative steps of nick translation in order to completely remove primer RNA. Finally, while elongation rates are under dynamic dNTP control, maturation rates are buffered against changes in dNTP concentrations.

Keywords

DNA polymerase delta; FEN1; PCNA; Okazaki Fragment maturation; toolbelt; quench-flow kinetics; replication rate

In eukaryotes, Okazaki fragment synthesis is initiated by DNA polymerase α-primase, which creates a 20–30 base primer initiated by approximately 7–10 nucleotides of RNA[1]. A conserved and highly regulated process synthesizes lagging strand DNA from these primers, and removes the Pol α-primase synthesized RNA from each of the ~50 million Okazaki fragments synthesized in mammalian cells, forming continuous double-stranded DNA upon nick ligation[2]. Many different DNA structures are formed during Okazaki fragment synthesis and maturation, and improper processing of these intermediates is a major cause of

Correspondence should be addressed to P.M.B. (; Email: burgers@biochem.wustl.edu)

AUTHOR CONTRIBUTIONS

J.S. and P.B. designed experiments and analyzed data. J.S. performed all experiments. Manuscript was written by J.S. and P.B.

COMPETING FINANCIAL INTERESTS

The authors declare no competing financial interests.

genome instability. Moreover, mutations can arise from the incomplete removal of Pol α-synthesized DNA[3].

DNA polymerase δ (Pol δ) performs the bulk of lagging strand DNA synthesis, extending Pol α primers until reaching the 5′-terminus of the preceding Okazaki fragment. In *Saccharomyces cerevisiae*, Pol δ is a three-subunit complex consisting of Pol3, Pol31, and Pol32[4]. The catalytic subunit Pol3 contains both the polymerase and the proofreading 3′–5′ exonuclease activities. Each subunit contains motifs that bind to the sliding clamp proliferating cell nuclear antigen (PCNA)[4–8]. When loaded onto primer termini by replication factor C (RFC) in an ATP-dependent reaction[9], PCNA increases the intrinsic processivity of Pol δ, allowing it to replicate hundreds of nucleotides in a single DNA binding event[10].

Since Okazaki fragments are initiated with Pol α-synthesized RNA, ligation cannot occur until initiator RNA is removed. This removal requires the joint activity of Pol δ and the structure-specific flap endonuclease I (FEN1). When Pol δ reaches the 5′-end of the previous Okazaki fragment, it continues replicating by limited displacement of the RNA primer, forming a 5′-flap, which is cut by FEN1. To completely remove the RNA primer, it has been proposed that iterative Pol δ strand displacement and FEN1 cleavage is required, a process termed nick translation[11,12]. The forward movement of Pol δ that results in strand displacement is countered by exonucleolytic activity of Pol δ that reverses this action; repetition of this cycle is known as idling. Idling supports maintenance of the nick position in the absence of other processing activities[13]. Without idling, unregulated strand displacement synthesis generates problematic long flaps that require alternative processing mechanisms[14], and can cause lethality when FEN1 activity is also compromised[15].

Okazaki fragment maturation, involving the action of Pol δ, FEN1, and DNA ligase I, is the best-studied example of a sequential, multi-enzyme process coordinated by PCNA. For maturation to occur efficiently, cooperation with PCNA must be tightly regulated, with enzymes exchanging access for DNA intermediates in a prescribed sequence. Debate remains concerning the mechanism of this cooperation. Due to its homotrimeric structure, it has been suggested that multiple enzymes may bind simultaneously to PCNA, each occupying a separate monomer; this is called the toolbelt model[16]. Biochemical evidence in support of toolbelt models has been reported in bacterial systems[16,17], and in archaea[18]. The alternative model presupposes dynamic binding to and dissociation from PCNA, resulting in sequential switching of partners. Use of engineered yeast PCNA heterotrimers provided biochemical evidence that nick translation does not absolutely require simultaneous binding of Pol δ and FEN1[19], but the methodology was insufficient to evaluate whether it actually occurs.

While the general pathway of Okazaki fragment maturation has been well established, several critical mechanistic steps have remained unresolved due to the low kinetic resolution of these studies. With the goal of better understanding how PCNA coordinates multiple enzymes during Okazaki fragment synthesis and maturation, we performed msec-resolution kinetic studies using a quench-flow apparatus. This analysis has revealed novel and unexpected insights into the regulation of 5′-flaps generation and processing. Furthermore,

our analysis provides evidence for the proposed toolbelt model of the Okazaki fragment maturation machinery.

RESULTS

PCNA increases the catalytic rate of Pol δ

The experimental design of our studies in the quench-flow apparatus is described in Online Methods. Unless otherwise noted, the exonuclease-deficient Pol δ-DV was used in all experiments to prevent degradation of DNA substrates[15]. We started with measuring the rate of incorporation of a single nucleotide by a preformed DNA-Pol δ complex (Fig. 1a); this rate constant is 9+/−1 sec^{-1} (Fig. 1b,c). Under our standard assay conditions, binding of the polymerase to DNA was saturated, and the dTTP concentration (250 μM) was near-saturation (Supplementary Fig. 1a,b). This rate constant is higher than observed in a previous analysis of Pol δ[20], but much slower than previously determined rates of replication by PCNA-Pol δ on RPA-coated ssDNA[21]. We first investigated whether inclusion of RPA enhanced the catalytic rate of Pol δ alone, but rather, RPA strongly inhibited incorporation (Supplementary Fig. 1e).

In contrast, when PCNA was loaded onto DNA, we observed that PCNA-Pol δ incorporated a single nucleotide at a rate too fast to be accurately determined in our apparatus (>300 sec^{-1}) (Fig. 1b,c). As polymerase was pre-bound to DNA in both experiments, the increase in rate constant is likely caused by intrinsic stimulation of the nucleotide incorporation rate by PCNA. Whether PCNA enhances the rate of the conformational change of the ternary polymerase-DNA-dNTP complex, or the chemical step, cannot be distinguished here[22]. Nevertheless, these novel data represent evidence that PCNA can actively influence the catalytic activity of a bound enzyme in addition to stabilizing it on DNA.

To determine how RPA influenced the rate of nucleotide incorporation by PCNA-Pol δ, reactions were initiated with dTTP and dATP, allowing the polymerase to incorporate 21 nucleotides (Fig. 1a,d, Supplementary Fig. 1d). For graphical representation, the median extension product was plotted as a function of time (Fig. 1e, description of analysis in Online Methods). At saturating dNTPs (Supplementary Fig. 1c), PCNA-Pol δ synthesized at a rate of ~340 nt/sec, with or without RPA (Fig. 1e), indicating that RPA does not affect replication of homopolymeric templates. On mixed-sequence DNAs, RPA aids in processivity by resolving secondary structures, however, this stimulation can also be accomplished by heterologous SSBs[23,24].

In yeast, dNTP concentrations are only 12–30 μM[25]. When extension reactions were performed using physiological levels of the four dNTPs, replication rates were reduced substantially, to 66 nt/sec, indicating that these rates are not maximized at normal cellular dNTP levels (Supplementary Fig. 1f,g). This is advantageous for fidelity purposes, as proofreading of errors is more efficient at subsaturating dNTPs[26]. Furthermore, rNTPs, present at much higher concentrations than dNTPs, represent a discrimination challenge to DNA polymerases[25,27]. When both dNTPs and rNTPs were included at physiological concentrations, DNA synthesis by PCNA-Pol δ proceeded at a rate of 51 nt/sec (Supplementary Fig. 1f,g), which is compatible with rates of fork movement in yeast[28].

Strand displacement synthesis by Pol δ

We next observed Pol δ approaching the 5′-terminus of a model Okazaki fragment and initiating strand displacement synthesis. Previous experiments lacked the kinetic resolution to determine what occurs when Pol δ reaches the double-stranded block, and what features of the 5′-block determine the kinetics of this process[21,29]. We annealed the primer and a downstream oligonucleotide block to their corresponding templates (Fig. 2a,c), leaving either a 2 or 5-nucleotide gap between primer-terminus and block.

We will first focus on the substrate with a 2-nt gap and a RNA_8DNA_{19} block (Fig. 2a). Rapid-quench kinetic experiments with the complete system (RPA, PCNA, RFC, Pol δ-DV, AMP-CPP) were performed as described in Fig. 1a, but in the presence of all four dNTPs at saturation. Following reaction initiation with dNTPs, Pol δ rapidly extended the primer at 200–300 nt/sec. The fractional occupancy of the nick product and of each strand displacement product was plotted over time (Fig. 2b). The final nucleotide closing the gap into a nick was inserted at a rate ~50% that of the normal synthesis rate, indicating that the presence of the block is sensed by the polymerase. Pol δ stalled substantially at the nick position (designated as **0**), indicating that it cannot seamlessly initiate strand displacement. Furthermore, the observed rate of nucleotide incorporation slowed to 10–20% with each successive step that the polymerase invaded the duplex DNA, from 11.3+/−1.0 sec^{-1} for the first nucleotide displaced, to 1.4+/−0.2 sec^{-1} for the second, and 0.38+/−0.06 sec^{-1} for the third nucleotide. Thus, the nascent flap acts as a progressive molecular brake on the DNA polymerase, limiting formation of longer flaps. Furthermore, this progressive slowdown is not the result of specific DNA or RNA sequences, but a consequence of the increasing length of the flap (Supplementary Fig. 2e–g). To extend the model-free fitting in Fig. 2b, we performed global kinetic fitting of these data to two different models (Supplementary Fig. 2a,b). These are discussed in detail in Supplementary Material, and their implications are considered further in the Discussion.

Given its function in Okazaki fragment maturation, Pol δ may have evolved the ability to displace RNA-DNA duplexes more readily than DNA-DNA duplexes. We investigated whether either the duplex stability or the sugar identity (RNA versus DNA) is the main determining factor for strand displacement capacity. We focused on the relative duplex stabilities of the 5′-proximal four base-pairs that initially block invasion by Pol δ (Fig. 2c). RNA-DNA and DNA-DNA duplex stabilities have been determined by nearest neighbor analysis[30]. The RNA-DNA duplex of Substrate I is more stable than the DNA-DNA duplex by 0.7 kcal/mol. Pol δ reached the nick at the same rate for both substrates (Fig. 2d,e, Supplementary Fig. 2c). However, the rate of release from the nick position and strand displacement synthesis proceeded faster for the DNA-DNA duplex than for the more stable RNA-DNA duplex substrate. When we reversed the duplex stabilities, with the DNA-DNA substrate being more stable, the RNA-block was displaced more rapidly than the DNA-block (Fig. 2c–e, Supplementary Fig. 2d). These data suggest that strand displacement rates are governed primarily by duplex stability rather than RNA *versus* DNA identity.

Pol δ idling at a nick

The studies above were carried out with exonuclease-deficient Pol δ-DV so that calculations of forward polymerization rates were uncomplicated by exonucleolytic degradation. Following limited strand displacement, wild-type Pol δ degrades DNA back to the nick position using its exonuclease in a process called idling[13]. To perform experiments with wild-type Pol δ, replication-competent complexes were assembled in the presence of dCTP and dGTP to prevent substrate degradation, and replication was initiated by addition of the four dNTPs (Fig. 3a). Fractional occupancies of select replication intermediates were compared to those measured with Pol δ-DV (Fig. 3b, Supplementary Fig. 3a). Replication up to the nick position was comparable for both forms of Pol δ. However, as the wild-type enzyme invaded the nick, it reversed using its exonuclease activity. As a result, the fraction of nick product did not decay, and compared to Pol δ-DV, flap products did not accumulate (Fig. 3b). An equilibrium distribution of products maintained by idling was reached within 500 msec. At equilibrium, the fractional occupancy of nick product was comparable to that of all flap products combined, suggesting that the rate of degradation is comparable to that of strand displacement of the first nucleotide (~10 s^{-1}). Rates of strand displacement by wild-type Pol δ are also governed by the stability of the block. A more stable block yielded an equilibrium distribution of extension products favoring the nick product and shorter flaps (Supplementary Fig. 3b,c,d).

FEN1 processes single-nucleotide flaps

We next reconstituted nick translation synthesis, requiring coordinated action of Pol δ and FEN1. Structural and mechanistic studies have shown that FEN1 does not simply cut 5′-flaps at their base as generally depicted, but binds a single 3′-extrahelical nucleotide into a specificity pocket, then cutting the 5′-strand one nucleotide into the dsDNA, which itself has become partially unpaired[31]. For a single nucleotide 5′-flap, which can equilibrate into a 3′-flap, the proposed cleavage mechanism is depicted in Fig. 4a. Previous studies showed that the major product produced by FEN1 during nick translation is a mononucleotide[12], presumably the result of cleavage following formation of a 1-nt flap by Pol δ. However, many have shown that the 1-nt flap is not the preferred substrate for FEN1; rather, FEN1 cuts double-flap structures with a single-nucleotide 3′-flap and a variable-length 5′-flap much more avidly[31–33]. Indeed, in our sequence context, double-flap substrates were cut faster than the single nucleotide flap (Supplementary Fig. 4i). Given the temporal resolution of our system, we can determine which strand displacement products provide substrates for FEN1. DNA substrates were labeled in various positions as indicated (Fig. 4b) to monitor different enzyme activities. Reactions were initiated with dNTPs together with FEN1 (Fig. 4b). Addition of FEN1 did not alter the rate at which Pol δ reached the nick position, nor the rate of +1 extension product formation (Fig. 4b, Supplementary Fig. 4a,b). However, the addition of FEN1 led to a very rapid decay of the +1 extension product, suggesting that FEN1 is acting upon this substrate (Fig. 4c).

We also monitored the production of FEN1 digestion products. The mononucleotide product predominated, but dinucleotides and trinucleotides were also formed (Supplementary Fig. 4c). The 1-nt cleavage product was formed with kinetics that lagged behind the formation of the +1 displacement product but prior to formation of the +2 displacement product (Fig. 4c),

indicating that the 1-nt cleavage product results from the displacement of a single nucleotide. If re-equilibration of the single nucleotide 5′-flap into a 3′-flap is a prerequisite for FEN1 activity, re-equilibration must occur at a time scale faster than cutting (>5 sec^{-1}). Two and three-nucleotide products resulted from processing of longer flaps that accumulated at later times (Supplementary Fig. 4d). Efficient flap cleavage relies on the interaction between PCNA and FEN1. The PCNA-defective mutant FEN1-p^{34} was strongly compromised in cutting flaps generated by PCNA-Pol δ (Fig. 4d, Supplementary Fig. 5e).

The prediction from these studies is that relative rates of strand displacement synthesis through sequences with different stabilities determine the distribution of FEN1 products. This is indeed what we observed; on our most stable substrate (Substrate III), strand displacement synthesis proceeded much slower than on the standard substrate (Supplementary Fig. 2f,g), and FEN1-products longer than the mononucleotide were negligible (Supplementary Fig. 4e,f,g). From these sets of data, we conclude that the major FEN1 substrate during nick translation is a single-nucleotide flap and not the double-flap that is more active in FEN1 cutting.

Coupling strand displacement to FEN1 action

A central proposal to the current view of nick translation is its coupled, reiterative nature, i.e. that multiple cycles of strand displacement and FEN1 cutting of predominantly 1-nt flaps removes the initiator RNA. As such, we predict that: first, FEN1 cuts iteratively at every position in the downstream oligonucleotide, in effect producing a ladder of products; second, that the degradation of the downstream oligonucleotide should match the extension of the primer oligonucleotide. To visualize all intermediates of FEN1 cutting, we labeled the 3′-end of the blocking oligonucleotide (Fig. 4b). Indeed, we observed a ladder of downstream oligonucleotides resulting from regular and reiterative FEN1 cutting. To examine polymerase-FEN1 coupling, the median primer length of products replicated past the nick position was compared to the median length of 3′-labeled oligonucleotides cut by FEN1 (Fig. 4b,e). When plotted, the slopes are nearly equivalent, with the median primer length increasing at ~5 nt/sec and the median downstream oligonucleotide degrading at ~4 nt/sec. This inverse relationship suggests a tight coupling of strand displacement and FEN1 nuclease activity to perform nick translation.

If polymerization during nick translation were rate limiting, a decrease in dNTP concentrations from saturating to physiological levels should decrease the nick translation rate to ~25%, as observed with unimpeded elongation (Supplementary Fig. 1g). A nick translation assay was carried out at physiological dNTP concentrations. Primer elongation rates during the linear range of nick translation were comparable at both saturating and physiological dNTP concentrations (Supplementary Fig. 4h), indicating that other steps during nick translation are likely rate limiting.

Experimental evaluation of the PCNA toolbelt model

Interaction with PCNA allows Pol δ to replicate ssDNA processively, but it remains unresolved to what extent PCNA-Pol δ can perform processive strand displacement synthesis, and furthermore, whether a stable PCNA-Pol δ-FEN1 complex exists that

performs processive nick translation. To determine whether PCNA-Pol δ can processively replicate through a typical Okazaki fragment primer (~7–10 nucleotides), we used heparin to trap free Pol δ that had dissociated from DNA (Fig. 5a). In the absence of PCNA, 10 μg/ml heparin completely inhibited Pol δ even when prebound to DNA (Fig. 5a, lanes 1,2). A second control experiment showed that pre-trapped Pol δ could not bind PCNA-DNA, and replication was inhibited (lanes 9,10). However, when Pol δ was pre-bound to PCNA-DNA, challenge with heparin upon initiation with dNTPs did not cause a decrease in strand displacement products after 5 sec, and we observed only a partial decrease after 20 sec (lanes 3,4 and 5,6), indicating that the complex is processive at the time-scale during which nick translation normally occurs. Processive strand displacement synthesis occurred through either DNA or RNA blocks, and at saturating or physiological dNTP levels (Fig. 5a, Supplementary Fig. 5a,b).

Second, we asked whether FEN1 also acted processively during nick translation. Since heparin inhibited FEN1 under all conditions (data not shown), we used an oligonucleotide trap substrate with a structure representing the optimal substrate for FEN1 (Supplementary Fig. 5e). This trap did not inhibit strand displacement synthesis by Pol δ (Fig. 5b, lanes 1–4). When, in a control experiment, FEN1 was pre-bound to the oligonucleotide trap prior reaction initiation with dNTPs, no products longer than the expected strand displacement products were observed (lanes 3,4 and 9,10), indicating that the trap did not inhibit strand displacement synthesis, but did inhibit FEN1. Also, pre-incubation of FEN1 with the trap blocked cleavage of a pre-formed flap-containing DNA (Supplementary Fig. 5e). However, when FEN1 was allowed to assemble onto the DNA-PCNA-Pol δ complex prior to addition of dNTPs with the DNA trap, very long extension products were formed, consistent with FEN1 acting processively during multiple cycles of nick translation (Fig. 5b, lanes 5,6 and 7,8). Processivity of nick translation was not absolute, since more efficient nick translation was observed in the absence of the trap, which allowed reloading of dissociated FEN1. One caveat of this experiment is that, because the DNA trap does not trap Pol δ, we formally cannot exclude the possibility that some polymerase dissociated and rebound during nick translation, even while FEN1 remained bound. However, since FEN1 remained processive, a DNA-PCNA-Pol δ-FEN1 complex must exist to advance nick translation.

These processive activities are completely dependent upon the interaction of FEN1 with PCNA since they were abrogated when the PCNA interaction-defective mutant FEN1-p was used (Supplementary Fig. 5c). Stable FEN1 binding to PCNA during nick translation did not depend on the form of polymerase used, since both exonuclease-deficient Pol δ-DV and wild-type Pol δ showed processive nick translation (Fig. 5b, Supplementary Fig. 5d). In sum, these data provide evidence that the quaternary DNA-PCNA-Pol δ-FEN1 complex performs efficient and processive nick translation.

DISCUSSION

Our high-resolution kinetic analysis has illuminated novel aspects of the basic steps of Okazaki fragment synthesis and maturation. Analysis of the DNA-Pol δ complex yielded the surprising result that the presence of PCNA greatly accelerated the observed incorporation rate of Pol δ (Fig. 1). This finding was surprising because the leading strand Pol ε shows a

high rate of incorporation in the absence of PCNA (~200–300 nt/sec), comparable to that of PCNA-Pol δ[35]. Furthermore, the orthologous bacteriophage T4 DNA polymerase shows a full catalytic rate of ~400 sec^{-1} in the absence of its PCNA-like replication clamp[36]. Thus, Pol δ shows two unique PCNA-stimulated activities, catalysis and processivity.

Our analysis focused on strand displacement synthesis by Pol δ and on nick translation, asking which activities could act in synergy to restrict flap sizes. When the polymerase enters an RNA-DNA or DNA-DNA block and initiates strand displacement synthesis, a progressive molecular brake is applied to the polymerase. Reduction of base-pairing energetics at the block alleviates the severity of the molecular brake. We show here that this can be accomplished by introducing less stable sequences at the block site (Fig. 2), but it can also be accomplished by reducing the salt concentration or raising the assay temperature[21], or even by mechanical pulling on the displaced strand, as shown by single-molecule techniques[37].

Our modeling of strand displacement synthesis kinetics do not currently allow us to conclusively point to a specific molecular mechanism explaining the progressive slowing of the polymerase. Either of the two models described in Supplementary Fig. 2a,b are consistent with our observations. It is possible that nucleotide insertion by Pol δ is progressively inhibited by the growing flap (Model 1), or that during strand displacement synthesis, the enzyme equilibrates between an extension competent form and an incompetent form (Model 2), or a combination of both. Model 1 does not sufficiently describe our data, because it does not contain steps in which Pol δ switches from its polymerase to exonuclease domain (idling, Fig. 3), or in which it releases the primer terminus, allowing FEN1 to act (nick translation, Fig. 4). Even though several rates in Model 2 remain poorly defined, we believe that this model has merit because it incorporates these additional steps necessary for nick translation.

Several studies, including ours (Supplementary Fig. 4i) indicate that the 1-nt flap is not the optimal FEN1 substrate[31,33]. Yet this structure is cut most frequently because it is the substrate presented to FEN1 during nick translation; the rate with which the 2-nt flap is produced from the 1-nt flap is generally lower than that of FEN1 cutting (Fig. 4c). However, if 2-nt or longer flaps are made, albeit infrequently, the increased rate with which they are cut by FEN1 should ensure that flaps generally do not grow to a dangerously long size (Fig. 6).

PCNA's homotrimeric structure has the potential to serve as a binding platform for multiple enzymes simultaneously (the toolbelt model). Previous studies have shown that two functional PCNA monomers are sufficient for full Pol δ activity[19]. Since FEN1 binds only a single PCNA monomer[38], Pol δ and FEN1 have the potential to remain simultaneously bound to a single PCNA during nick translation. Our data support the model that a quaternary DNA-PCNA-Pol δ-FEN1 complex performs processive nick translation synthesis. Evaluating the PCNA toolbelt model *in vivo* remains a challenge. The PCNA interaction defect in FEN1-p not only reduced nuclease recruitment to the emerging flap, but also prevented processive action by FEN1 during nick translation (Supplementary Fig. 5c). The latter defect prevents the toolbelt mechanism from operating. Remarkably, despite these

defects, FEN1-p (*rad27-p*) mutants show only marginal genetic instability phenotypes in yeast[34,39]. However, when redundant controls on excessive strand displacement synthesis are eliminated, such as in a Pol δ exonuclease-defective mutant, the *rad27-p* mutation can cause synthetic lethality[40]. At this point we are unable to attribute the genetic defect of the *rad27-p* mutant to either the recruitment or processivity defect of FEN-p.

We show that Pol δ processively performs strand displacement in the time-scale relevant for Okazaki fragment maturation (Fig. 5a); nick translation proceeds at a rate of ~5 nt/sec (Fig. 4e), suggesting that removal of RNA should generally be accomplished within two seconds. A previous report determined that Pol δ collision with the 5′-end of an Okazaki fragment reduces the affinity of the polymerase for DNA, designated “collision release”[24]. Since we find that the whole process should be complete within just a few seconds, our data do not disagree with that study, which was carried out at a time scale of minutes. Therefore, while the collision release model may be important under some circumstances, appreciable dissociation of Pol δ occurs too slowly to seriously affect nick translation. It could be argued that at lower, physiological dNTP concentrations, nick translation might occur at a reduced rate. However, we found this not to be the case (Supplementary Fig. 4h). These data suggest that steps other than primer elongation are rate limiting. Likely, these involve the consecutive steps of polymerase release, flap re-equilibration, FEN1 flap engagement, and cutting. Nucleotide levels in yeast are under dynamic control, e.g. responding to stress[41]. Our data suggest that while elongation rates are under strict dNTP control, maturation rates are buffered against changes in dNTP concentrations.

The focus of our study has been on Pol δ and FEN1, and their DNA-bound complex with PCNA. DNA ligase I, which completes the process has not been included in this study. In archaeal replication studies, a processive complex of polymerase, FEN1, and ligase with the heterotrimeric PCNA has been observed[18,42]. It is likely that the eukaryotic machinery works in a slightly different manner. Eukaryotic DNA ligase I also contains a PCNA-binding domain[43], one function of which is recruiting ligase to replication foci[44]. However, previous studies have shown that ligase acts distributively, and the position of ligation following RNA removal is largely dependent on ligase concentrations[21]. In yeast, acute depletion of DNA ligase allows nick translation to proceed up to the dyad of the nucleosome that has been assembled onto the completed lagging strand[45]. The analysis of these small fragments has provided valuable information regarding the limits that the cellular environment sets to nick translation by the PCNA-Pol δ-FEN1 complex.

ONLINE METHODS

Proteins

RPA[46], PCNA[47], RFC[48], FEN1 and the PCNA-interaction defective FEN1-p (F346G F347A)[34] were purified from *E. coli* overexpression systems, while Pol δ and the exonuclease-defective Pol δ-DV (D520V) were purified from yeast overexpression systems[49].

DNA substrates

All oligonucleotides were obtained from Integrated DNA Technologies (Coralville, IA) and were purified by either polyacrlyamide gel electrophoresis or high-pressure liquid chromatography prior to use. Sequences of oligonucleotides are listed in Supplementary Table 1. Primer29, used in all studies was either 5′-^{32}P-labeled with T4 polynucleotide kinase (New England BioLabs) and [γ-^{32}P] ATP, or ordered with a 5′-Cy3 fluorophore. No difference in primer extension activity was observed between the different labeling methods. Primer extension DNA templates were made by annealing labeled primer and blocking oligonucleotides to the template in a 0.8:2:1 ratio. 3′-labeled block templates were made by annealing primer and labeled block to the template in a 1.4:0.8:1 ratio, respectively. 5′-labeled block templates were made by annealing primer and labeled block to the template in a 0.8:1.4:1 ratio, respectively. To hybridize, oligonucleotides were heated to 75 °C in 100 mM NaCl and cooled slowly to room temperature. After hybridization, streptavidin was added in 2-fold molar excess to template-primer substrates. All substrates, except those in Supplementary Fig. 4i, contain 3′- and 5′-biotin-streptavidin bumpers to support stable PCNA loading by RFC[21]. DNA concentrations in replication assays were calculated according to the labeled oligonucleotide concentration. In strand displacement templates, the gap between the primer-terminus and the 5′-block was limited to either two or five nucleotides in order to maximize synchrony of replicating complexes initiating strand displacement synthesis.

Replication reactions

All replication experiments were performed in a buffer containing 20 mM Tris-HCl, pH 7.8, 1 mM Dithiothreitol, 200 μg/ml bovine serum albumin, 8 mM $Mg(OAc)_2$, and 100 mM NaCl. Unless otherwise noted, standard reaction conditions were: 10 nM DNA template, 40 nM Pol δ (DV or wild-type), 30 nM PCNA, 15 nM RFC, 100 μM α,β-methyleneadenosine 5′-triphosphate (AMP-CPP) for RFC-catalyzed loading of PCNA, and 50 nM RPA for studies in Fig. 1, and 25 nM RPA for all other studies. PCNA loading by RFC is an ATP-dependent process[9]. However, because ATP is also a substrate for Pol δ[25], it could not be used in our system. Therefore, we replaced ATP with AMP-CPP, which acts efficiently in PCNA loading but cannot be incorporated by the DNA polymerase. The Pol δ-DV (D520V) mutant was used in most reactions, unless otherwise noted. This exonuclease-deficient mutant prevents degradation of oligonucleotide substrates prior to reaction initiation[15].

Reactions were initiated with 250 μM each dNTP, unless otherwise noted. In select experiments, physiological concentrations of the four dNTPs and rNTPs were used; physiological dNTP concentrations in *S. cerevisiae* are 16 μM dATP, 14 μM dCTP, 12 μM dGTP, and 30 μM dTTP, and the rNTP concentrations are 3 mM ATP, 0.5 mM CTP, 0.7 mM GTP, 1.7 mM UTP[25].

All reactions except those in Fig. 5 and Supplementary Fig. 5 were performed in a quenched-flow apparatus (KinTek RQF-3) maintained at 30 °C with a circulating water bath. DNA templates pre-incubated with Pol δ, with and without other protein factors (PCNA, RFC, RPA) and AMP-CPP as indicated. The pre-assembled complexes were loaded into one loop of the quenched-flow apparatus. The second loop contained initiating nucleotides (and

FEN1 when present) in reaction buffer. Reactions were initiated by mixing equal volumes and quenched with 200 mM EDTA and 0.2% SDS. DNA products were ethanol precipitated in the presence of 10 μg/ml glycogen, and resolved on 12–20% denaturing polyacrylamide gels. Gels containing ^{32}P-labeled DNAs were dried and subjected to PhosphorImager analysis. Gels containing Cy3-labeled DNAs were visualized by detecting Cy3 fluorescence using a Typhoon-Trio (GE healthcare). All quantification was carried out using ImageQuant software (GE healthcare).

Each reaction was performed at least twice under identical conditions. For exact repeats of strand displacement reactions, variations in fractional occupancy of specific products did not exceed 0.1, even at the shortest time points. At time points exceeding 50 msec, curves from identical replicates were indistinguishable. Observed rates in all figures are reported to highlight qualitative differences between reaction conditions, with standard errors reported for the fits of individual time courses.

Median analysis

The median analysis method was used to generate the data presented in Fig. 1e, Fig. 4e, Supplementary Fig. 1c,g, and Supplementary Fig. 4h. This methodology takes into consideration that complexes do not move with perfect synchrony through the available template, and is described in detail in the legend to Supplementary Fig. 6.

Supplementary Material

Refer to Web version on PubMed Central for supplementary material.

Acknowledgments

The authors thank J. Majors, R. Galletto, and T. Lohman for critical discussions during the progress of this work, and C. Stith for protein purification. This work was supported in part the US National Institutes of Health (GM032431 to P.B) and from the U.S.-Israel Binational Science Foundation (2013358 to P.B.)

References

1. Perera RL, et al. Mechanism for priming DNA synthesis by yeast DNA polymerase alpha. Elife. 2013; 2:e00482. [PubMed: 23599895]
2. Balakrishnan L, Bambara RA. Eukaryotic lagging strand DNA replication employs a multi-pathway mechanism that protects genome integrity. J Biol Chem. 2010; 286:6865–70. [PubMed: 21177245]
3. Reijns MA, et al. Lagging-strand replication shapes the mutational landscape of the genome. Nature. 2015
4. Gerik KJ, Li X, Pautz A, Burgers PM. Characterization of the two small subunits of Saccharomyces cerevisiae DNA polymerase delta. J Biol Chem. 1998; 273:19747–19755. [PubMed: 9677405]
5. Bermudez VP, MacNeill SA, Tappin I, Hurwitz J. The influence of the Cdc27 subunit on the properties of the Schizosaccharomyces pombe DNA polymerase delta. J Biol Chem. 2002; 277:36853–36862. [PubMed: 12124382]
6. Lu X, et al. Direct interaction of proliferating cell nuclear antigen with the small subunit of DNA polymerase delta. J Biol Chem. 2002; 277:24340–24345. [PubMed: 11986310]
7. Netz DJ, et al. Eukaryotic DNA polymerases require an iron-sulfur cluster for the formation of active complexes. Nat Chem Biol. 2011; 8:125–32. [PubMed: 22119860]

8. Acharya N, Klassen R, Johnson RE, Prakash L, Prakash S. PCNA binding domains in all three subunits of yeast DNA polymerase delta modulate its function in DNA replication. Proc Natl Acad Sci U S A. 2011; 108:17927–32. [PubMed: 22003126]
9. Tsurimoto T, Stillman B. Functions of replication factor C and proliferating cell nuclear antigen: functional similarity of DNA polymerase accessory proteins from human cells and bacteriophage T4. Proc Natl Acad Sci USA. 1990; 87:1023–1027. [PubMed: 1967833]
10. Chilkova O, et al. The eukaryotic leading and lagging strand DNA polymerases are loaded onto primer-ends via separate mechanisms but have comparable processivity in the presence of PCNA. Nucleic Acids Res. 2007; 35:6588–97. [PubMed: 17905813]
11. Bhagwat M, Nossal NG. Bacteriophage T4 RNase H removes both RNA primers and adjacent DNA from the 5′- end of lagging strand fragments. J Biol Chem. 2001; 276:28516–28524. [PubMed: 11376000]
12. Stith CM, Sterling J, Resnick MA, Gordenin DA, Burgers PM. Flexibility of eukaryotic Okazaki fragment maturation through regulated strand displacement synthesis. J Biol Chem. 2008; 283:34129–40. [PubMed: 18927077]
13. Garg P, Stith CM, Sabouri N, Johansson E, Burgers PM. Idling by DNA polymerase delta maintains a ligatable nick during lagging-strand DNA replication. Genes Dev. 2004; 18:2764–2773. [PubMed: 15520275]
14. Kang YH, Lee CH, Seo YS. Dna2 on the road to Okazaki fragment processing and genome stability in eukaryotes. Crit Rev Biochem Mol Biol. 2010; 45:71–96. [PubMed: 20131965]
15. Jin YH, et al. The 3′–>5′ exonuclease of DNA polymerase delta can substitute for the 5′ flap endonuclease Rad27/Fen1 in processing Okazaki fragments and preventing genome instability. Proc Natl Acad Sci USA. 2001; 98:5122–5127. [PubMed: 11309502]
16. Indiani C, McInerney P, Georgescu R, Goodman MF, O'Donnell M. A sliding-clamp toolbelt binds high- and low-fidelity DNA polymerases simultaneously. Mol Cell. 2005; 19:805–15. [PubMed: 16168375]
17. Kath JE, et al. Polymerase exchange on single DNA molecules reveals processivity clamp control of translesion synthesis. Proc Natl Acad Sci U S A. 2014; 111:7647–52. [PubMed: 24825884]
18. Beattie TR, Bell SD. Coordination of multiple enzyme activities by a single PCNA in archaeal Okazaki fragment maturation. EMBO J. 2012; 31:1556–67. [PubMed: 22307085]
19. Dovrat D, Stodola JL, Burgers PM, Aharoni A. Sequential switching of binding partners on PCNA during in vitro Okazaki fragment maturation. Proc Natl Acad Sci U S A. 2014; 111:14118–23. [PubMed: 25228764]
20. Dieckman LM, Johnson RE, Prakash S, Washington MT. Pre-steady state kinetic studies of the fidelity of nucleotide incorporation by yeast DNA polymerase delta. Biochemistry. 2010; 49:7344–50. [PubMed: 20666462]
21. Ayyagari R, Gomes XV, Gordenin DA, Burgers PM. Okazaki fragment maturation in yeast. I. Distribution of functions between FEN1 AND DNA2. J Biol Chem. 2003; 278:1618–1625. [PubMed: 12424238]
22. Johnson KA. Role of induced fit in enzyme specificity: a molecular forward/reverse switch. J Biol Chem. 2008; 283:26297–301. [PubMed: 18544537]
23. Burgers PMJ. Saccharomyces cerevisiae Replication factor C. II. Formation and activity of complexes with the proliferating cell nuclear antigen and with DNA polymerases delta and epsilon. J Biol Chem. 1991; 266:22698–22706. [PubMed: 1682322]
24. Langston LD, O'Donnell M. DNA polymerase delta is highly processive with PCNA and undergoes collision release upon completing DNA. J Biol Chem. 2008
25. Nick McElhinny SA, et al. Abundant ribonucleotide incorporation into DNA by yeast replicative polymerases. Proc Natl Acad Sci U S A. 2010; 107:4949–54. [PubMed: 20194773]
26. Kunkel TA, Sabatino RD, Bambara RA. Exonucleolytic proofreading by calf thymus DNA polymerase delta. Proc Natl Acad Sci U S A. 1987; 84:4865–9. [PubMed: 3474631]
27. Sparks JL, et al. RNase H2-initiated ribonucleotide excision repair. Mol Cell. 2012; 47:980–6. [PubMed: 22864116]
28. Raghuraman MK, et al. Replication dynamics of the yeast genome. Science. 2001; 294:115–121. [PubMed: 11588253]

29. Podust VN, Podust LM, Muller F, Hubscher U. DNA polymerase delta holoenzyme: action on single-stranded DNA and on double-stranded DNA in the presence of replicative DNA helicases. Biochemistry. 1995; 34:5003–5010. [PubMed: 7711022]
30. Sugimoto N, Nakano S, Yoneyama M, Honda K. Improved thermodynamic parameters and helix initiation factor to predict stability of DNA duplexes. Nucleic Acids Res. 1996; 24:4501–5. [PubMed: 8948641]
31. Tsutakawa SE, et al. Human flap endonuclease structures, DNA double-base flipping, and a unified understanding of the FEN1 superfamily. Cell. 2011; 145:198–211. [PubMed: 21496641]
32. Kaiser MW, et al. A comparison of eubacterial and archaeal structure-specific 5′-exonucleases. J Biol Chem. 1999; 274:21387–94. [PubMed: 10409700]
33. Kao HI, Henricksen LA, Liu Y, Bambara RA. Cleavage specificity of Saccharomyces cerevisiae flap endonuclease 1 suggests a double-flap structure as the cellular substrate. J Biol Chem. 2002; 277:14379–14389. [PubMed: 11825897]
34. Gomes XV, Burgers PMJ. Two modes of FEN1 binding to PCNA regulated by DNA. EMBO J. 2000; 19:3811–3821. [PubMed: 10899134]
35. Ganai RA, Osterman P, Johansson E. Yeast DNA polymerase catalytic core and holoenzyme have comparable catalytic rates. J Biol Chem. 2015; 290:3825–35. [PubMed: 25538242]
36. Capson TL, et al. Kinetic characterization of the polymerase and exonuclease activities of the gene 43 protein of bacteriophage T4. Biochemistry. 1992; 31:10984–94. [PubMed: 1332748]
37. Manosas M, et al. Mechanism of strand displacement synthesis by DNA replicative polymerases. Nucleic Acids Res. 2012; 40:6174–86. [PubMed: 22434889]
38. Chapados BR, et al. Structural basis for FEN-1 substrate specificity and PCNA-mediated activation in DNA replication and repair. Cell. 2004; 116:39–50. [PubMed: 14718165]
39. Gary R, et al. A novel role in DNA metabolism for the binding of Fen1/Rad27 to PCNA and implications for genetic risk. Mol Cell Biol. 1999; 19:5373–5382. [PubMed: 10409728]
40. Jin YH, et al. The multiple biological roles for the 3′–5′-exonuclease of DNA polymerase d require switching between the polymerase and exonuclease domains. Mol Cell Biol. 2005; 25:461–471. [PubMed: 15601866]
41. Chabes A, et al. Survival of DNA damage in yeast directly depends on increased dNTP levels allowed by relaxed feedback inhibition of ribonucleotide reductase. Cell. 2003; 112:391–401. [PubMed: 12581528]
42. Cannone G, Xu Y, Beattie TR, Bell SD, Spagnolo L. The architecture of an Okazaki fragment-processing holoenzyme from the archaeon Sulfolobus solfataricus. Biochem J. 2015; 465:239–45. [PubMed: 25299633]
43. Vijayakumar S, et al. The C-terminal domain of yeast PCNA is required for physical and functional interactions with Cdc9 DNA ligase. Nucleic Acids Res. 2007; 35:1624–37. [PubMed: 17308348]
44. Montecucco A, et al. DNA ligase I is recruited to sites of DNA replication by an interaction with proliferating cell nuclear antigen: identification of a common targeting mechanism for the assembly of replication factories. EMBO J. 1998; 17:3786–3795. [PubMed: 9649448]
45. Smith DJ, Whitehouse I. Intrinsic coupling of lagging-strand synthesis to chromatin assembly. Nature. 2012; 483:434–8. [PubMed: 22419157]
46. Henricksen LA, Umbricht CB, Wold MS. Recombinant replication protein A: expression, complex formation, and functional characterization [published erratum appears in J Biol Chem 1994 Jun 10;269(23):16519]. J Biol Chem. 1994; 269:11121–11132. [PubMed: 8157639]
47. Eissenberg JC, Ayyagari R, Gomes XV, Burgers P. Mutations in yeast proliferating cell nuclear antigen define distinct sites for interaction with DNA polymerase delta and DNA polymerase epsilon. Mol Cell Biol. 1997; 17:6367–6378. [PubMed: 9343398]
48. Gomes XV, Gary SL, Burgers PM. Overproduction in Escherichia coli and characterization of yeast replication factor C lacking the ligase homology domain. J Biol Chem. 2000; 275:14541–14549. [PubMed: 10799539]
49. Fortune JM, Stith CM, Kissling GE, Burgers PM, Kunkel TA. RPA and PCNA suppress formation of large deletion errors by yeast DNA polymerase delta. Nucleic Acids Res. 2006; 34:4335–4341. [PubMed: 16936322]

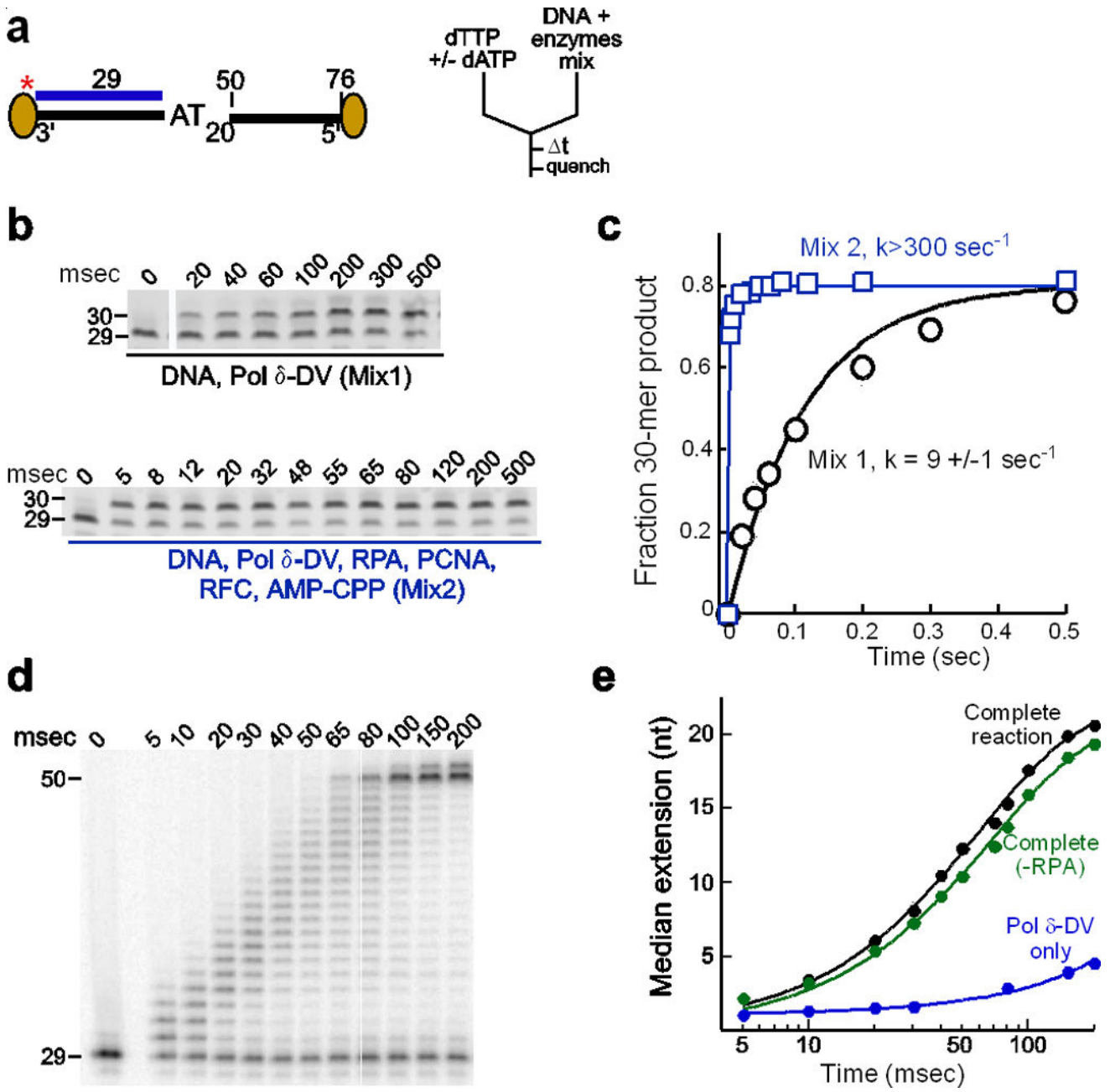

Figure 1. PCNA stimulates catalytic rate of Pol δ

(**a**) DNA substrate and rapid-quench experimental setup. (**b**) Time-courses of single nucleotide incorporation by Pol δ-DV. Reactions contained standard DNA and enzyme concentrations as described in Online Methods, with or without accessory proteins as defined in “Mixes”. Reactions were initiated with 250 μM dTTP. (**c**) Quantification of **b**. Time courses were fit to single exponentials, representative of first-order kinetics. (**d**) Replication of a homopolymeric DNA by PCNA-Pol δ. Reaction contained all accessory proteins, and was initiated with 250 μM each dTTP and dATP, allowing extension of 29-mer to a 50-mer product. (**e**) Quantification of **d** and of Supplementary Fig. 1d. Median extension was determined as described in detail in Online Methods. Complete reaction

(black) contains DNA and Pol δ-DV, RPA, PCNA, RFC, and AMP-CPP. Green curve contains all components except RPA, and blue curve contains only DNA and Pol δ-DV.

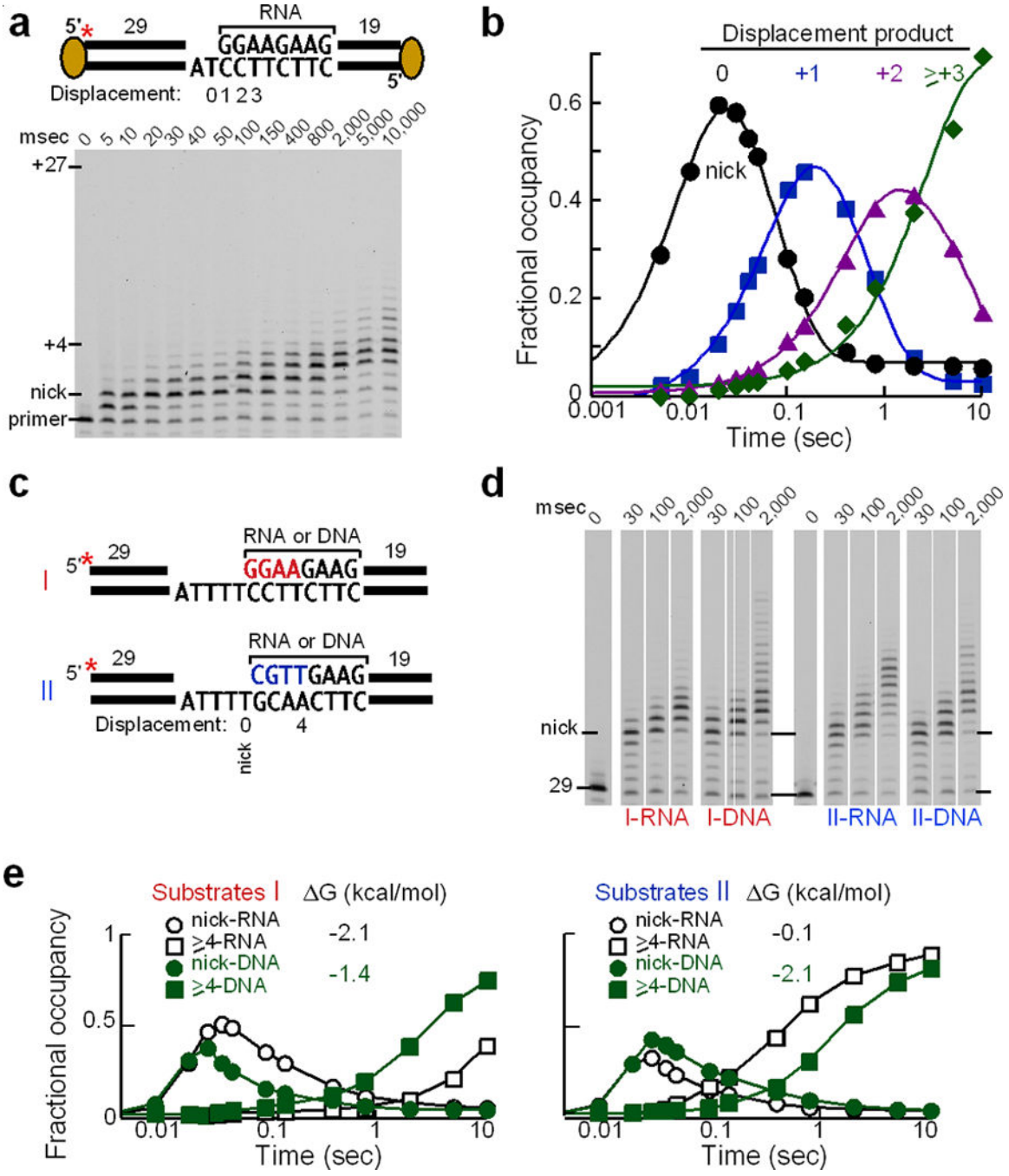

Figure 2. Strand displacement synthesis by PCNA-Pol δ

(**a**) Top, model of DNA substrate. Strand displacement positions (nick=**0**) are indicated. Blocking oligonucleotide initiated with RNA_8. Bottom, gel of replication products. (**b**) Quantification of **a**. Fractional occupancy of strand displacement intermediates. Nick position and strand displacement products of one, two, and three and greater nucleotides are shown. Time courses fit to the sum of two exponentials, to model formation and decay of intermediates, with the exception of the +3 and greater (green) curve, which was fit to a single exponential. (**c**) Strand displacement substrates used in **d**, containing a five nucleotide

gap. Substrate I (red) and Substrate II (blue) differ in four nucleotides at the 5′-end of the blocking oligonucleotide. Blocks initiated with either RNA_8 or DNA_8 as indicated. (**d**) Select time points of strand displacement time courses; full time courses shown in Supplementary Fig. 2c,d. (**e**) Fractional occupancy of select replication products from **d**. Nick position (circles) and intermediates four nucleotides and greater past nick (squares) are plotted. Free energy ΔG values of the 5′-terminal 4-bp duplexes were calculated as described[30].

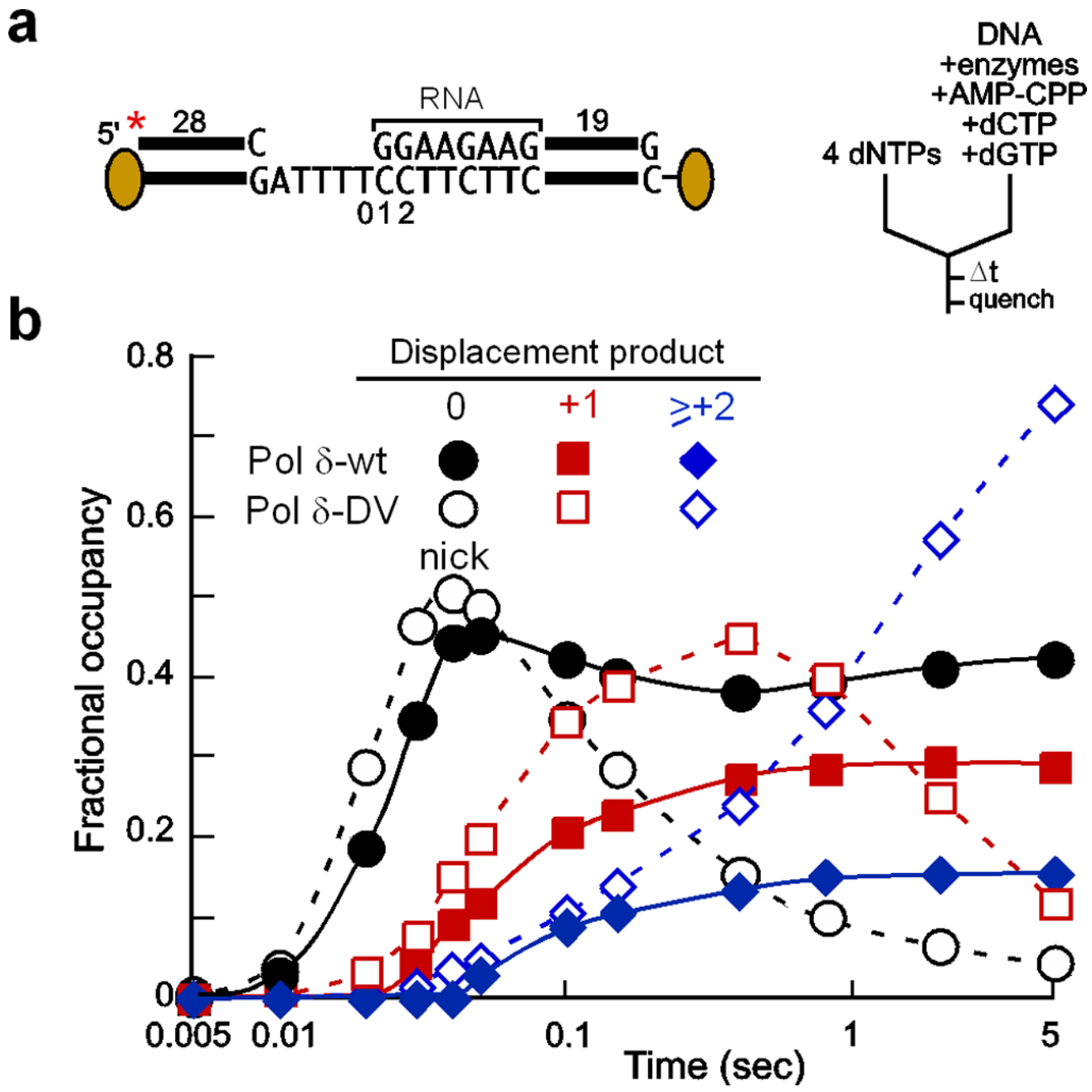

Figure 3. Strand displacement synthesis and idling by wild-type Pol δ

(**a**) DNA substrate I, RNA block was preincubated with RPA, PCNA, RFC, AMP-CPP, Pol δ under standard assay conditions, and with 150 μM dCTP & dGTP to prevent degradation of oligonucleotides by wild-type Pol δ. (**b**) Strand displacement product distribution of Pol δ-DV and Pol δ-wt. Quantification of Supplementary Fig. 3a (wild-type) and Supplementary Fig. 2c (DV). Fractional occupancies of nick position, +1 product, and +2 and greater products past nick are plotted.

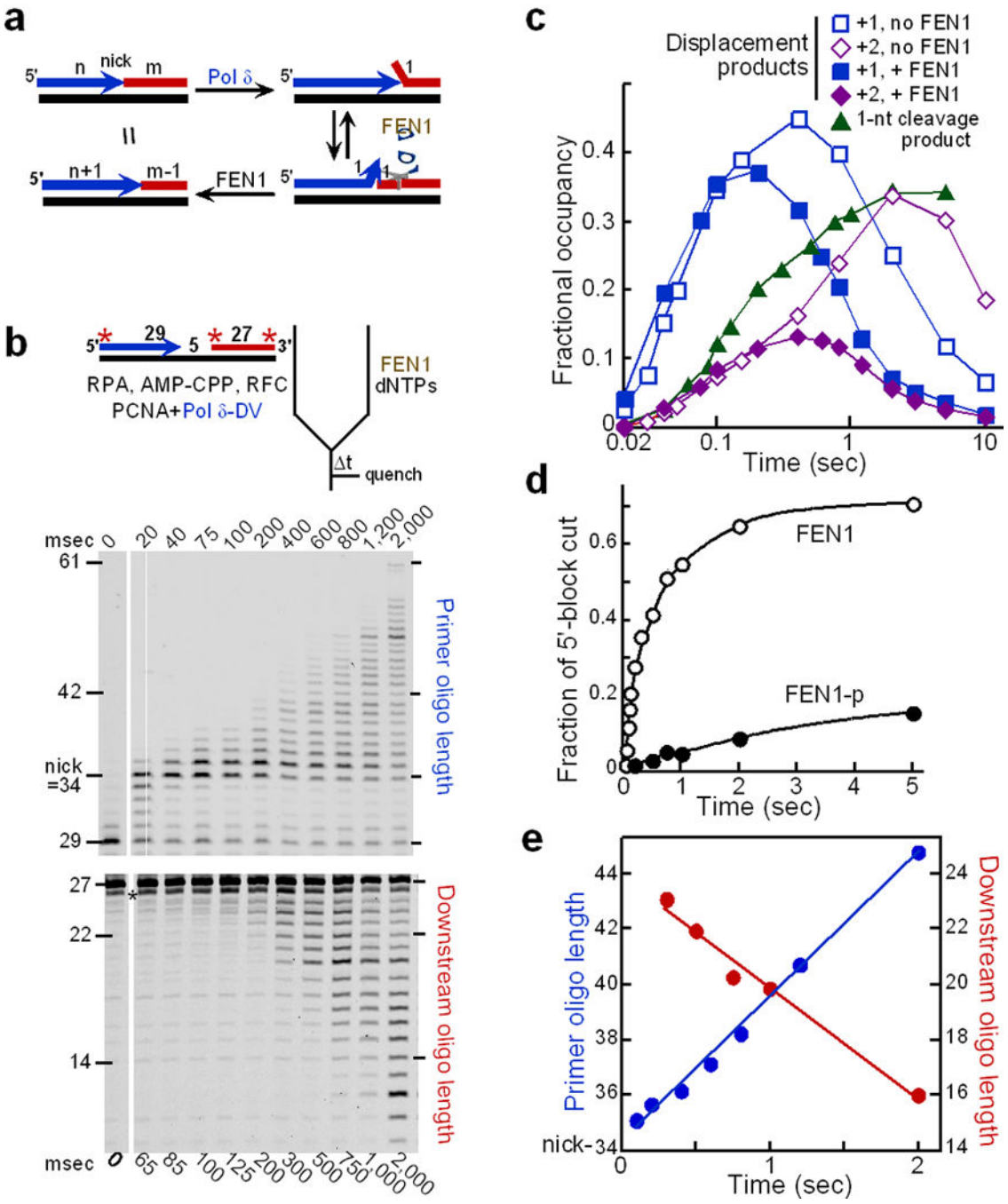

Figure 4. Nick translation by Pol δ and FEN1

(**a**) Model for FEN1 mechanism in nick translation. (**b**) Top, design of nick translation assay. DNA templates (Substrate I-RNA block) contained a 5′-primer label, a 5′-block label, or a 3′-block label. 5′-primer labeling reports extension by Pol δ. 5′-block labeling measures the first product released by FEN1. 3′-block labeling measures how far FEN1 has cut into block. PCNA-Pol δ complex was pre-formed and reactions initiated with dNTPs plus 40 nM FEN1. Top gel shows primer extension (5′-labeled primer), and bottom gel shows FEN1 cleavage of block (3′-labeled block). *, non-specific band. (**c**) Quantification of **b** (top gel, +FEN1),

Supplementary Fig. 2c (Substrate I-RNA, no FEN1), and Supplementary Fig. 4c (fraction of 1-nt product). (**d**) 5′-labeled block products cut by FEN1 or FEN1-p (40 nM). Fraction cut is sum of 1, 2, and 3-nt products. (**e**) Quantification of **b**. Median extension product past nick position (blue, left y-axis) derived from top gel, and median cleavage product (red, right y-axis) derived from bottom gel. Analysis of the FEN1-generated products (bottom gel) was started at the 300 msec time point, at which significant FEN1-mediated degradation had occurred. Accurate quantification of earlier time point products was not feasible because of the presence of contaminants in the oligonucleotide (*).

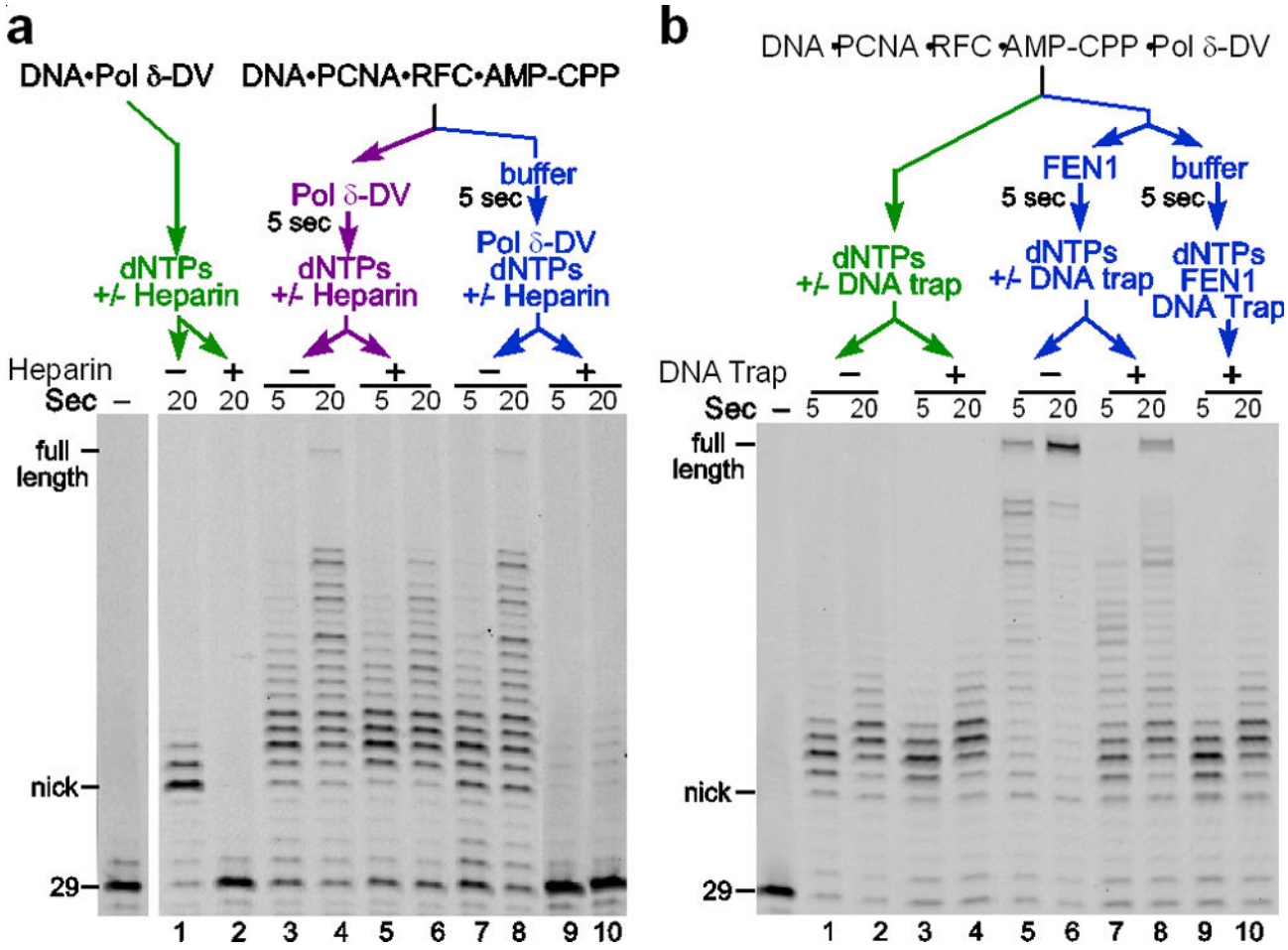

Figure 5. Processivity of the nick translation machinery

(**a**) Strand displacement synthesis by PCNA-Pol δ on Substrate I-DNA block. Reactions were initiated with 250 μM dNTPs with or without 10 μg/ml heparin. (**b**) Nick translation assay; forced single turnover of 40 nM FEN1. DNA template was Substrate I-RNA block. Reactions were initiated with 250 μM dNTPs, with or without 6 μM oligonucleotide FEN1 trap (Supplementary Fig. 4i, bottom DNA).

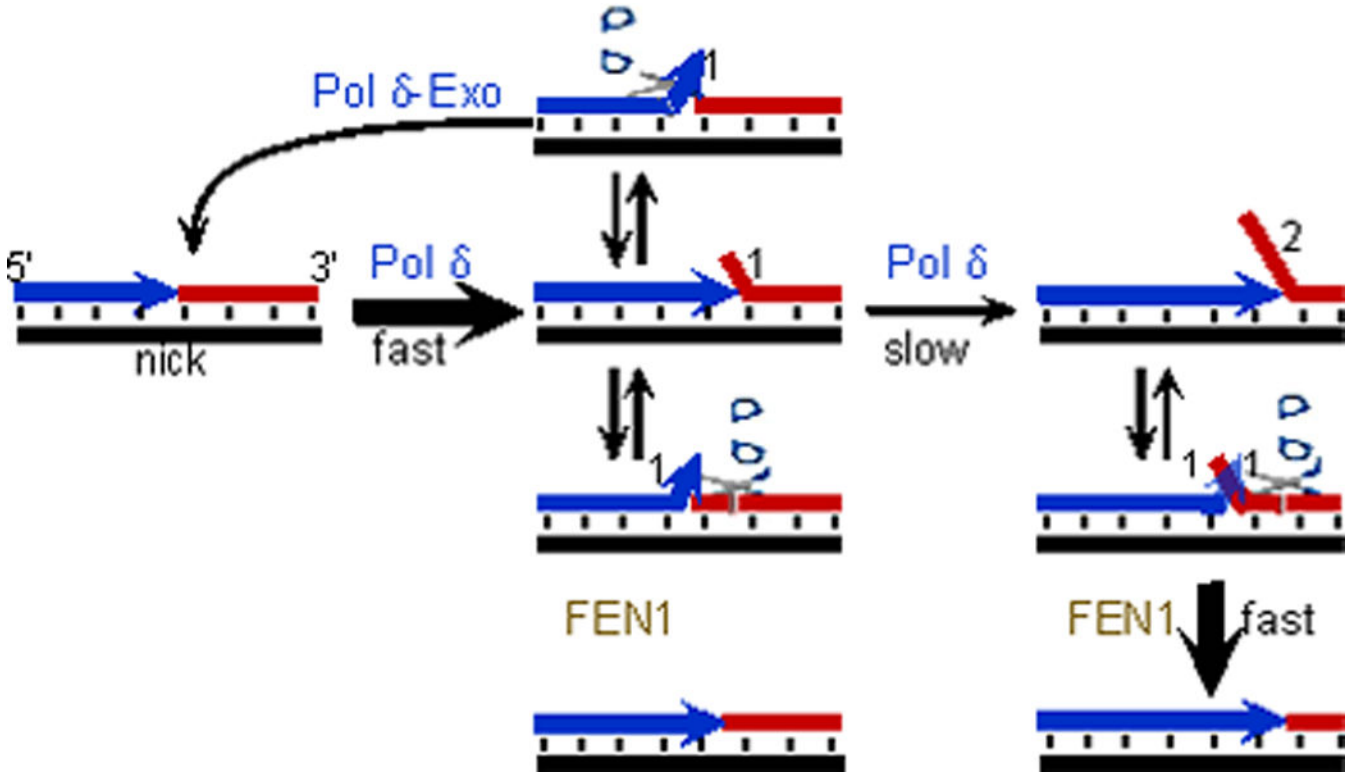

Figure 6. Model for short flap maintenance and nick translation
See text for details